

## Double-Plate Cloud-Chamber Study of $V^0$ Particles: Classification and Related Results\*†‡

ISHWAR C. GUPTA, W. Y. CHANG, AND ALLEN L. SNYDER  
*Physics Department, Purdue University, Lafayette, Indiana*

(Received February 10, 1956; revised manuscript received December 26, 1956)

Two rectangular cloud chambers have been used independently for the study of  $V^0$  particles. A total of 39 347 pairs of good pictures was obtained, in which there were 3439 penetrating showers. 254  $V^0$  events have been found in these pictures, of which 129 are shower-associated events. 102 out of these show clear association with nuclear interactions having measurable origins in the first or second plate or in the chamber roof, and have been analyzed according to the  $\alpha-\epsilon$  projection procedure supplemented with the ionization values. From the measured angles of the two decay products relative to the  $V^0$  particles, two alternative sets of ionizations of the decay products (for  $\theta^0$  and  $\Lambda^0$  particles) have been obtained with the help of  $\alpha-\epsilon$  diagrams and compared with the experimentally estimated ionizations. In this way 39  $V$  events have been classified as due to  $\theta^0$  particles, 23 as due to  $\Lambda^0$  particles, 11 as "nonclassified" events, and 13 as anomalous cases. After weighting the individual events for the detection efficiency, the numbers of  $\theta^0$  and  $\Lambda^0$  particles are found to be  $106 \pm 31$  and  $52 \pm 18$ , respectively. Distributions of the noncoplanarity angles show that both  $\theta^0$  and  $\Lambda^0$  decays are most probably of the two-body type. The angular distribution of the decay products of  $\theta^0$  particles in the rest system indicates a spin higher than 0 for  $\theta^0$  particles.

### I. INTRODUCTION

IN preliminary studies, little was known about the  $V^0$  particle. Therefore, identification of the decay products in each individual case was important. Supplemented with other measurements, information was thus deduced about the nature of the  $V^0$  particle and its decay scheme. Work of this kind was done sometimes by a magnet cloud chamber and sometimes by a multiplate cloud chamber.<sup>1</sup> However, it is well known that when these methods are used the percentage of measurable and hence analyzable events is usually very small. Therefore, in later studies when the types of  $V^0$  particles and their decay schemes are fairly well established, a simpler and more efficient method is desirable in order to accumulate high statistics within a reasonable period. High statistics are needed so that physical quantities involved can be determined more accurately and detailed features, some of which may yet be unknown, may be revealed more readily.

During the past year, our two rectangular cloud chambers<sup>2</sup> have been used independently to study the  $V^0$  events, and up to now a good number of cases has been obtained. This paper (to be called Part I) presents an analysis of many of these events, making use of the  $\alpha-\epsilon$  projection in conjunction with the estimated

ionization values of the decay products. After classification, the mean decay times of the  $\theta^0$  and  $\Lambda^0$  particles have also been determined according to a suitable statistical procedure; the methods of measurement and analysis, and the results for the mean decay times will be given and discussed in the following paper.<sup>3</sup>

### II. EXPERIMENTAL. GENERAL STATISTICS

#### 1. Experimental

As mentioned before, the two cloud chambers, which were used for the study of penetrating showers,<sup>2</sup> have been set up independently to investigate  $V^0$  events since the early summer of 1954. One chamber has been placed in the third floor (under one roof) and the other in the first floor of the physics building. The two units have had practically the same arrangements of the lead plates, counters, and photographic equipment. Each chamber (inside dimensions  $16 \times 16 \times 14$  inches) contains three lead plates ( $10 \times 11$  inches each) having thicknesses  $2$ ,  $\frac{5}{8}$ , and  $\frac{3}{8}$  inches, respectively, as shown in Fig. 1. The spacings for observing the particle tracks are about  $3$ ,  $3\frac{1}{2}$ ,  $3\frac{1}{2}$ , and  $2\frac{1}{2}$  inches at the front edges of the lead plates. A twofold coincidence telescope (second tray protected by anticoincidence counters) and a shower detector ( $c_3$ ,  $c_4$ ; counters separated by  $\frac{1}{4}$  inch Pb) have been used to trigger the chamber for penetrating showers, the number of particles entering the chamber via the telescope being about 60 per minute. A Recordak Microfile camera (lens at about 47 inches from the front edge of the central plate) and a front-coated mirror (perpendicular to the chamber) have been used for taking pictures.

In order to apply the procedure of the  $\alpha-\epsilon$  projection (see Sec. III) for classifying the  $V^0$  events, the origin of the nuclear interaction and hence of the  $V^0$  particle has to be well determined. The two-inch Pb plate was used

\* Material in this paper forms part of the material of Ishwar C. Gupta's Dissertation for the Degree of Doctor of Philosophy to be submitted to the Graduate School at Purdue University.

† Supported in part by the Purdue Research Foundation.

‡ Preliminary results reported at the 1955 Thanksgiving Meeting of the American Physical Society held at Chicago [Phys. Rev. **100**, 1264(A) (1955)]; also at the Washington Meeting, April, 1956 [Bull. Am. Phys. Soc. Ser. II, **1**, 186 (1956)].

<sup>1</sup> For earlier work, see references given in *Progress in Cosmic Ray Physics*, edited by J. G. Wilson (North-Holland Publishing Company, Amsterdam, 1952 and 1954), Vol. I and Vol. II. For more recent work, see, for example, Leighton, Wanlass, and Anderson, Phys. Rev. **89**, 148 (1953); Thompson, Buskirk, Etter, Karmark, and Rediker, Phys. Rev. **90**, 329 (1953); Fretter, May, and Nakada, Phys. Rev. **89**, 168 (1953); Bridge, Peyrou, Rossi, and Safford, Phys. Rev. **91**, 362 (1953).

<sup>2</sup> G. del Castillo, Ph.D. thesis, Purdue University, 1954 (unpublished); Phys. Rev. **98**, 1163(A) (1955).

<sup>3</sup> Snyder, Chang, and Gupta, following paper [Phys. Rev. **106**, 149 (1957)], hereafter referred to as Part II.

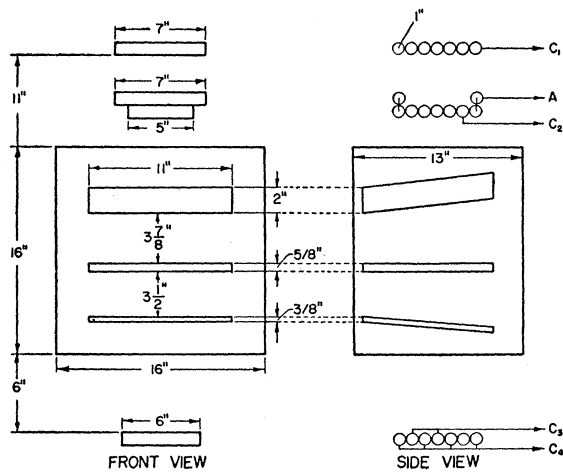


FIG. 1. Experimental arrangement.

inside the chamber with the intention that many of the penetrating showers would be produced in this plate; thus the origin could be better located than if it were outside the chamber. The two thinner plates ( $\frac{5}{8}$  and  $\frac{3}{8}$  inch) have been employed to define a  $V^0$  event. In order to be qualified as a real  $V^0$  event, at least one prong must pass through either plate without multiplication or without being scattered at an angle larger than  $20^\circ$ . However, when a  $V^0$  event has an angle larger than  $30^\circ$  and its prongs do not show much multiple scattering in the gas, it is to be taken also as a real  $V^0$  event, even if neither of its prongs passes through a plate. These conditions are designed to reduce the probability of mistaking electron-positron pairs for real  $V^0$  events. The  $V^0$  events in the last gas space have been ignored entirely. This is partly because the large-angle criterion, which could be used to select real  $V^0$  events in the last gas space only, would provide a bias against narrow-angle  $V^0$  events, and partly because this space was not always very well illuminated.

## 2. General Statistics

Up to now a total of 39 347 pairs of *good* pictures has been taken. It has been found that 1711 penetrating

TABLE I. Distribution of penetrating showers and  $V^0$  events.<sup>a-c</sup>  
Total number of good paired pictures taken = 39 347.

	No. of penetrating showers	No. of $V^0$ events associated with P. S.	No. of $V^0$ events unassociated with P. S.
P. S. origin outside	329	13	
P. S. origin in Plate I	1711	85	
P. S. origin in Plate II	1399	31	
Total	3439	129	125

<sup>a</sup> No. of  $V^0$  events per penetrating shower =  $129/3439 \sim 1/26$ .

<sup>b</sup> P. S. stands for penetrating showers.

<sup>c</sup> One backward  $V^0$  event is also included in the 125 events of the last column.

showers were produced in the first plate (2 inch) and 1399 in the second plate ( $\frac{5}{8}$  inch). The ratio of these two figures is smaller than would be expected from that of the thicknesses of the two Pb plates. This is chiefly due to the fact that in many pictures cascade penetrating showers occurred, i.e., in many cases when a shower was produced in the first plate, one or more showers were produced in the second plate by one or more particles of the first shower.

A total of 254  $V^0$  events has been found from all the pictures taken and examined. Many of these were associated with penetrating showers, produced either outside or inside the chamber, of uncertain origins, and many more with no observable nuclear events; all of these uncertain events had to be discarded for analysis though a great number of them were perfect  $V^0$  events. Only 102 events out of the 129 shower-associated  $V^0$  events have shown clear association with the nuclear interactions having origins measurable in the first or second Pb plate (6 of the 102 with the penetrating shower origins in the chamber roof) and are suitable for analysis. The distribution of the penetrating showers and the  $V^0$  events is presented in Table I. The results of analysis of these  $V^0$  events are summarized in Table IV.

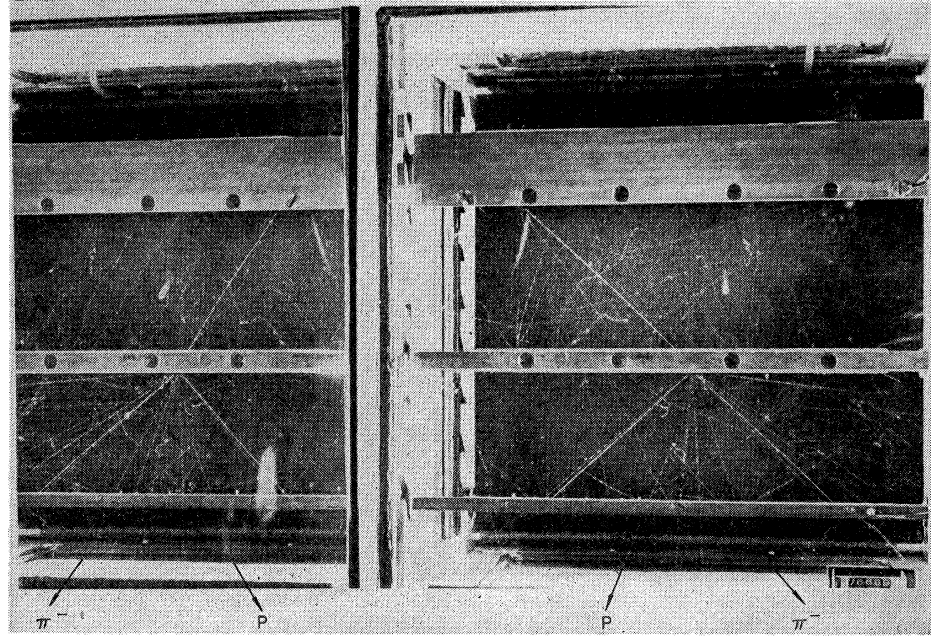
A picture which has two  $V^0$  events has been observed. In the case (34-9630) the two  $V^0$  events appear to have been associated with one single penetrating shower origin and both have been classified as probably due to the decay of two  $\theta^0$  particles. Of course, there is no way to determine whether the two  $\theta^0$  particles are produced in a single elementary act (which we shall assume in the discussion later) or in two separate interactions. These two have been included in the  $V^0$  events analyzed as shown in Table III.

Figure 2 shows, as an example, a cloud chamber picture (in both views) of a  $V^0$  event (30-6869), where the nuclear interaction takes place in the second Pb plate and the  $V^0$  event occurs in the third gas space. Particle (1) makes an angle  $\phi_1 = 8.75^\circ$  with the line of flight and has an estimated ionization  $I_1/I_{\min} = 2.5$ , while particle (2) has  $\phi_2 = 55.2^\circ$  and estimated ionization  $I_2/I_{\min} = 2$ . According to the analysis to be discussed, particle (1), which is on the left-hand side in the direct view, is identified as a proton and particle (2) as a pion. Hence this  $V^0$  event is classified as a  $\Lambda^0$  decay event.

## III. PRINCIPLE OF CLASSIFICATION

In general the principle employed in classifying a  $V^0$  event is based on the conservation laws of energy and momentum supplemented by the ionization-momentum relationship and the Lorentz transformation between the laboratory system and the rest system of the decaying particle. If one assumes a two-body decay, the eight quantities  $M$ ,  $m_1$ ,  $m_2$ ,  $P$ ,  $p_1$ ,  $p_2$ ,  $\phi_1$ , and  $\phi_2$  are to be determined from the three equations representing the two conservation laws. For example, if we assume

FIG. 2. Example of the production of a  $V^0$  particle in the second lead plate. The particle decays in the third gas space. The decay products are identified as proton ( $p$ ) and  $\pi^-$ .  $\Lambda^0$  has a momentum,  $P=681$  Mev/c. Event (30-6869).



a known decay scheme, i.e.,  $M$ ,  $m_1$ , and  $m_2$  and are able to measure, say  $\phi_1$  and  $\phi_2$ , the angles of the decay products with the direction of the  $V^0$  particle, then we can calculate  $P$ ,  $p_1$ , and  $p_2$ . The ionizations,  $I_1$  and  $I_2$ , are thus found from the ionization-momentum curves and can be then compared with the experimentally estimated ionizations of the two decay products. If the agreement is not satisfactory, an alternative decay scheme may be tried. Thus, a cloud chamber containing a producing plate and a plate to suggest the nature of the decay prongs should provide sufficient data for the analysis of the event. This *direct* procedure of classifying the event, however, would become tedious and perhaps practically impossible if it had to be applied to a large number of events, of which  $\phi_1$ ,  $\phi_2$ ,  $I_1$ , and  $I_2$  are measured.

A convenient way of employing the conservation laws to display the experimental results has been developed, from a more general point of view, by Podolanski and Armenteros<sup>4</sup> along lines similar to the considerations of previous workers.<sup>5</sup> They have suggested the use of the variables  $\alpha$ ,  $\epsilon$ , and  $1/P$  which are better suited for the analysis than the directly measured physical quantities. By using these variables, the two-body decay may be written as<sup>4</sup>

$$\frac{\epsilon^2}{(M/P)^2} + \frac{(\alpha - \alpha^*)^2}{1 + (M/P)^2} = \epsilon^{*2}, \quad (1)$$

<sup>4</sup> T. Podolanski and R. Armenteros, *Phil. Mag.* 45, 13 (1953).

<sup>5</sup> Some of the properties of these new variables have been employed by earlier workers in the analysis of their  $V^0$  events, for examples, Armenteros *et al.*, Thompson *et al.*, Fretter *et al.*; see footnote 1 for references.

where

$$\alpha = (p_{1l} - p_{2l})/P = \sin(\phi_2 - \phi_1)/\sin\phi, \quad 2(a)$$

$$\epsilon = 2p_t/P = 2 \sin\phi_1 \sin\phi_2/\sin\phi, \quad 2(b)$$

$$\alpha^* = (m_1^2 - m_2^2)/M^2, \quad \epsilon^* = 2p^*/M. \quad (3)$$

Here  $p^*$  is the momentum of either of the decay products in the rest system and thus depends only on  $M$ ,  $m_1$ , and  $m_2$ .

In the analysis of our  $V^0$  events, we assume that the majority of the  $V^0$  particles decay according to either of the following decay schemes:

$$\Lambda^0 \rightarrow p + \pi^- + 37 \text{ Mev}, \quad (4)$$

$$\theta^0 \rightarrow \pi^+ + \pi^- + 210 \text{ Mev}. \quad (5)$$

The constants involved in these two decay schemes are listed in Table II. In the  $\alpha$ - $\epsilon$  projection, Eq. (1) represents a family of confocal ellipses, corresponding to different values of  $P$ . Figures 3(a) and 3(b) show such ellipses for the above two decay schemes, respectively. The  $\alpha$ - $\epsilon$  plots are extremely useful in calculating the two alternative sets (corresponding to  $\theta^0$  and  $\Lambda^0$ )

TABLE II. Values of constants  $\alpha^*$ ,  $\epsilon^*$ , and  $p^*$ .<sup>a-c</sup>

Constants $V^0$ particles	$M$	$m_1$	$m_2$	$\alpha^*$	$\epsilon^*$	$p^*$
	$\Lambda^0$	1116	938	139	0.69	0.18
$\theta^0$	493	139	139	0	0.82	204

<sup>a</sup> All masses and momenta are in Mev.

<sup>b</sup> Velocity of light is taken as unity.

<sup>c</sup>  $M_{\Lambda^0} = (2182 \pm 2)m_e$ ;  $M_{\theta^0} = (965 \pm 10)m_e$ ;  $M_{\pi} = (273 \pm 0.7)m_e$ .

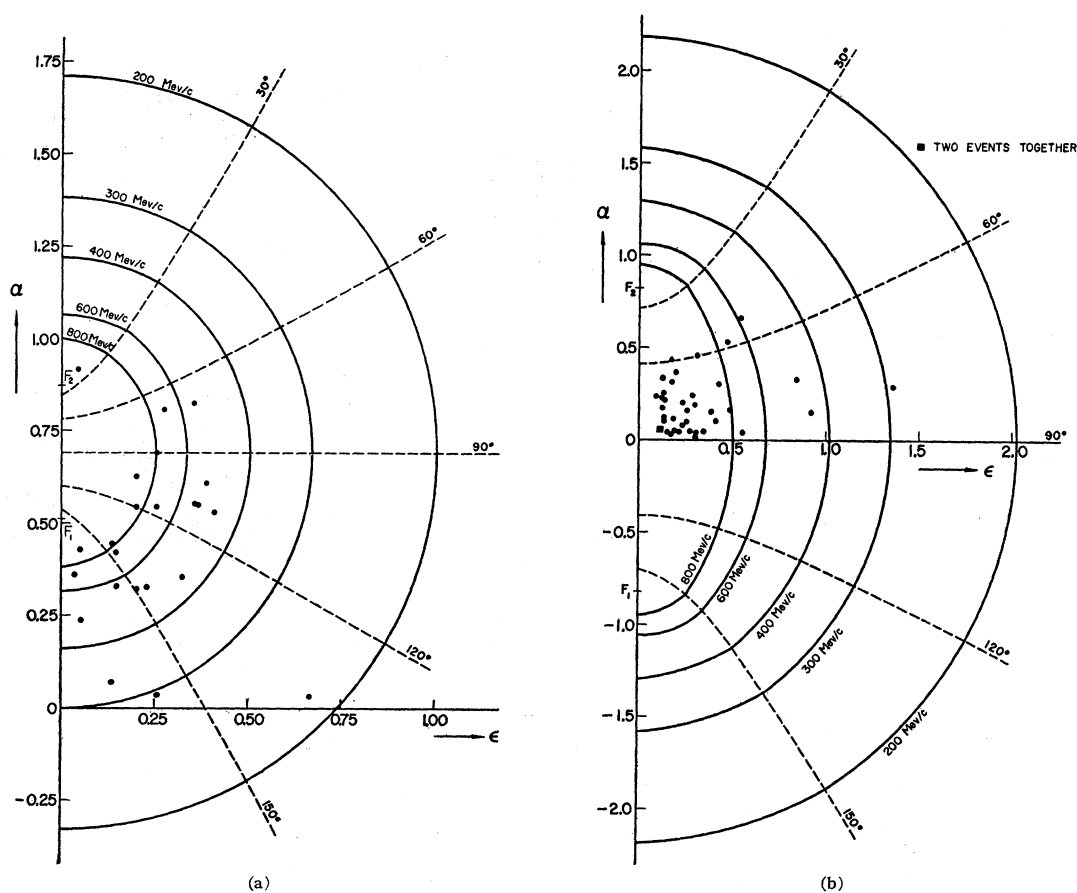


FIG. 3. (a) The  $(\alpha-\epsilon)$  diagram for the  $\Lambda^0$  particle. The ellipses in the diagram are the  $\alpha-\epsilon$  projections with  $P$ , the momentum of  $\Lambda^0$  particle, as parameter, whereas the hyperbolas are the projections with  $\theta$ , the angle of emission of the decay products in the rest system, as parameter. Foci  $F_1, F_2$  are on the  $\alpha$  axis at  $(\alpha^* - \epsilon^*)$  and  $\alpha^* + \epsilon^*$ , respectively. The points representing the observed events have been used to determine the angle  $\theta$  and the momentum of the  $\Lambda^0$  particle. (b) The  $(\alpha-\epsilon)$  diagram for the  $\theta^0$  particle. The ellipses in the diagram are the  $\alpha-\epsilon$  projections with  $P$ , the momentum of the  $\theta^0$  particle, as parameter, whereas the hyperbolas are the  $\alpha-\epsilon$  projections with  $\theta$ , the angle of emission of the decay products in the rest system, as parameter. Foci  $F_1, F_2$  are on the  $\alpha$  axis at  $-\epsilon^*$  and  $\epsilon^*$ . The points representing the observed events have been used to determine the angle  $\theta$  and the momentum of the  $\theta^0$  particle.

particles) of  $p_1$  and  $p_2$  and hence of the ionizations, which can be then compared with the experimentally estimated ionizations.

Equation (1) with  $\theta$ , the angle of emission of particle (1) in the rest system, as a parameter, is given by

$$\frac{(\alpha - \alpha^*)^2}{\cos^2 \theta} - \frac{\epsilon^2}{\sin^2 \theta} = \epsilon^{*2}. \quad (6)$$

Hence, the curves  $\theta = \text{const}$  (i.e.,  $p_t = \text{const}$ ) are a set of confocal hyperbolas with the same foci as the ellipses. These hyperbolas have been used for testing the isotropy of emission of the decay products in the rest system of the  $V^0$  particle, as will be discussed later.

#### IV. MEASUREMENTS

##### 1. Reprojection

Each  $V^0$  event and the associated penetrating shower origin were examined with a three-dimensional repro-

jection unit,<sup>6</sup> which has the same geometrical configuration as the camera-mirror-cloud chamber arrangement in the experiment. The distance from the projector and angles of rotation of the screen about two perpendicular axes can be read from scales.

A mapping of each picture containing a  $V^0$  event associated with a penetrating shower was made in the following manner. After projecting the picture, the screen was oriented so as to bring into coincidence the two projected images of the  $V^0$  event and those of a few high-energy penetrating shower particles. This whole picture including the related illumination edges was carefully traced over a sheet of semitransparent paper attached firmly on to the screen. The illumination edges were determined beforehand and formed the boundaries of the uniformly illuminated region in the

<sup>6</sup> A. Snyder, M.S. thesis, Purdue University, 1955 (unpublished); see also footnote 2. This is one of two units designed and built for examining the penetrating shower pictures taken with the two cloud chambers placed one above the other.

chamber. The penetrating shower origin was taken as the center of gravity of the intersection points (on the  $V^0$  plane extended) of the shower particles. The region over which the intersection points are scattered is approximated by a circle and is referred to henceforth as the "circle of uncertainty." The mapping of the illumination edges together with the  $V^0$  event is necessary for the measurement of the potential decay length to be discussed in Part II.

## 2. Angles, $\phi_1$ and $\phi_2$ , and the Ionizations, $I_1$ and $I_2$

The angles  $\phi_1$  and  $\phi_2$ , were measured from the mapping according to the convention  $\phi_1 < \phi_2$ . The values of  $\phi_1$  and  $\phi_2$  are shown in Table III. Errors in the measurements of angle come mainly from uncertainty in the location of the penetrating shower origins. The magnitude of the uncertainty in the angles varied from one event to another. In the classification of the  $V^0$  events, the effect of this uncertainty on the calculation of  $p_1$ ,  $p_2$  and hence on the corresponding ionization was taken into careful consideration in each individual case.

The ionization of the prongs of the  $V^0$  event was estimated in the usual way. Each of the estimated ionization values given in Table III represents an average over independent estimates by three people.

## 3. Angle $\delta$

In the present analysis of the  $V^0$  events it is assumed that the decay schemes involve only two secondary particles. Therefore the plane of each  $V^0$  event should contain the origin of the  $V^0$  particle. To check this coplanarity, the angle  $\delta$  between the line of flight of the  $V^0$  particle and its decay plane was measured. To fix the line of flight of the  $V^0$  particle, the origin of the penetrating shower was determined by extending the high-energy particle tracks backward and was indicated by a pointer at that place. The screen was then adjusted, so as to bring the apex of the  $V^0$  event on the diametrical axis of the screen and to make the two images of the  $V^0$  event coincident. Now rotating the screen about its diametrical axis until it touched the pointer, representing the origin of the penetrating shower, the angle  $\delta$  was read off the scale. The mean value of  $\delta$  for each event is listed in the last column of Table III.

## V. CLASSIFICATION, RESULTS, AND DISCUSSION

### 1. $\alpha - \epsilon$ Ionization Procedure

For each  $V^0$  event, the values of  $\alpha$  and  $\epsilon$  can be calculated from the measured angles,  $\phi_1$  and  $\phi_2$ , by using Eqs. (2a) and (2b). Let  $f_1$  and  $f_2$  be the distances of this point to the foci of an  $\alpha - \epsilon$  plot. Then the angle of emission,  $\theta$ , in the rest system of the  $V^0$  particle is given by

$$\cos\theta = (f_1 - f_2)/2\epsilon^*. \quad (7)$$

Since the transverse momentum is unchanged under Lorentz transformation,

$$p_1 = p^* \sin\theta / \sin\phi_1; \quad p_2 = p^* \sin\theta / \sin\phi_2. \quad (8)$$

Values of  $\epsilon^*$  and  $p^*$  for the two decay schemes to be used in classification are given in Table II. Therefore, for each event two alternative sets of  $f_1$  and  $f_2$  can be obtained from Figs. 3(a) and 3(b), respectively, and hence two sets of  $p_1$  and  $p_2$ . Consequently, two alternative sets of ionizations,  $I_1/I_{\min}$  and  $I_2/I_{\min}$ , can be found from the ionization-momentum curves and be compared with the experimentally estimated values. In this way, one of the two decay schemes may be decided. The results of classification are presented in Table III, where the three pairs of ionizations (two calculated and one observed) are also given. In the process of classification, the effects of the uncertainty in the measurements of  $\phi_1$  and  $\phi_2$  on the values of  $\alpha$  and  $\epsilon$  (and hence on  $p_1$  and  $p_2$ ) have been carefully considered in each case, and the location of  $p_1$  and  $p_2$  in the momentum-ionization curves has also been noted.

The following conditions have been generally used to define the degree of definiteness in the classification:

(1) A classification (into  $\theta^0$ ,  $\Lambda^0$ , or anomalous event) is called "*certain*," if the ionization agreement is good and the classification is not changed when the initial point of the line of flight is shifted from the center to the opposite extreme points<sup>7</sup> of the "circle of uncertainty" (see Sec. IV, 1).

(2) A classification is called "*starred*" if the ionization agreement becomes poor when the initial point of the line of flight is shifted to either extreme point of the "circle of uncertainty," or if the observed ionization values are only near to that of the event as classified.

(3) An "*anomalous*" event is one whose observed pair of ionizations do not agree with either one of the two calculated pairs, no matter how the line of flight is drawn within the "circle of uncertainty."

(4) A "*nonclassified*" event is one whose observed pair of ionizations appear to agree with both calculated pairs, or one which would switch from a  $\theta^0$ -like to a  $\Lambda^0$ -like event when the line of flight is drawn differently within the "circle of uncertainty."

For the purpose of measurement, the smaller angle has been taken as  $\phi_1$  so that  $\phi_1 < \phi_2$ . In reality, for  $\theta^0$  decay events both signs of  $\alpha$  are equally probable, and a change in the sign of  $\alpha$  does not actually affect the values of  $p_1$  and  $p_2$ . This is obviously not true in the case of  $\Lambda^0$  decay [see Figs. 3(a) and 3(b)]. In the case of  $\Lambda^0$  decay events, the particle  $m_1$  (proton) has in general a smaller angle (due to larger momentum) than  $m_2$ , and hence  $\phi_1 < \phi_2$ , except when the  $\Lambda^0$  particle has very low energy. Therefore, it is necessary to try the negative value of  $\alpha$  only for those cases where one or both prongs have heavy ionization. Negative values of

<sup>7</sup> The  $\delta$  value of the  $V^0$  event may be taken as a useful check for the uncertainty in the  $\phi_1$  and  $\phi_2$  values, presuming the decay to be a two-body one.

TABLE III. Classification of the shower-associated  $V$  events.\*

Film and frame No.	$\phi_1$ deg	$\phi_2$ deg	$\alpha^b$	$\epsilon$	$\theta^0$		$\Lambda^0$		Observed		Classification	$\phi_1$ Mev/c	$\phi_2$ Mev/c	$\delta$ deg	$\pm(\Delta\delta)$ deg
					$I_1$ $I_{min}$	$I_2$ $I_{min}$	$I_1$ $I_{min}$	$I_2$ $I_{min}$	$I_1$ $I_{min}$	$I_2$ $I_{min}$					
11-2589	1.3	26.8	0.92	0.04	1	2.2	1.2	4.6	<2	4-6	$\Lambda^0$	1200	57	0	1
13-3472	1.6	3.4	0.36	0.04	1	1	3.5	1.1	3-4	<1.5	$\Lambda^0$	450	210	1.3	0.6
13-4007	10.0	19.0	0.32	0.23	1	1	5.4	1.2	5.5	1-3	$\Lambda^0$	330	170	2	0.8
14-4411	13.3	39.0	0.55	0.37	1	1	4.0	1.4	2-5	<1.5	$\Lambda^0$	410	150	0	0.6
15-4953	6.0	14.5	0.42	0.15	1	1	2.7	1.0	1.5-3	<1.5	$\Lambda^0$	530	220	0.3	0.6
15-5010	9.5	29.5	0.54	0.26	1	1	2.6	1.2	1.5-3	<1.5	$\Lambda^0$	550	180	3	1
15-5400	14.3	15.3	0.04	0.26	1	1	>14	1.4	10-15	1-3	$\Lambda^0$	160	140	0.5	1.1
16-5516	14.5	15.8	0.04	0.27	1	1	>14	1.2	1	<1.5	$\theta^0$	810	750	4	2
16-5583	17.3	45.5	0.53	0.47	1	1	6	1.4	1.5	1-2	$\theta^0$	580	240	4.7	1
16-6182	12.3	37.0	0.55	0.36	1	1	3.5	1.3	3-4	<2	$\Lambda^0$	450	160	3	1
17-6438	7.5	8.5	0.07	0.14	1	1	>14	1.4	12-15	<3	$\Lambda^0$	170	150	1	1.2
17-6595	12.0	14.0	0.08	0.23	1	1	9.2	1.2	1-2	1-2	$\theta^0$	980	840	1	1.3
17-6949	33.0	34.8	0.03	0.67	1	1	>>14	1.5	10-15	2	$\Lambda^0$	130	130	0.5	1
18-7359	38.8	47.5	0.15	0.92	1	1.7	>14	1.6	1	<2	$\theta^0$	320	120	0	1
19-8280	6.0	6.8	0.06	0.11	1	1	>14	1.5	1	1	$\theta^0$	1900	1700	0.5	1.3
22-0182	8.8	16.5	0.32	0.20	1	1	5.2	1.2	4	2	$\Lambda^0$	340	180	3	2
22-0411	22.3	29.5	0.16	0.48	1	1	>14	1.5	<1.5	<1.5	$\theta^0$	530	410	3	3
22-0649	6.5	16.5	0.44	0.17	1	1	2.7	1.1	1	1.5	$\theta^{0*}$	1500	620	3.5	1
23-1248	18.0	19.3	0.04	0.34	1	1	>>14	1.5	<1.5	<1.5	$\theta^0$	660	620	1	0.8
24-1725	18.3	24.0	0.15	0.38	1	1	12	1.2	1.5	1	$\theta^0$	640	490	4	4
24-1895	16.5	16.8	0.01	0.30	1	1	>>14	1.5	<1.5	<1.5	$\theta^0$	710	700	0.6	0.6
27-4019	7.5	24.0	0.54	0.20	1	1	2.1	1.1	<3	<1.5	$\Lambda^0$	670	210	4	2
28-4933	2.5	4.3	0.24	0.06	1	1	7.4	1.2	3	1	$\Lambda^{0*}$	280	170	1.8	0.4
29-6016	6.0	10.0	0.25	0.13	1	1	7.8	1.1	1	1	$\theta^0$	1900	1100	1.4	1.3
30-6394	6.5	12.8	0.33	0.15	1	1	3.2	1.0	4	1.5	$\Lambda^{0*}$	480	430	1	1
30-6794	9.5	10.0	0.03	0.17	1	1	>>14	1.6	<1.5	1	$\theta^0$	1200	1200	0.9	1
30-6869	8.8	55.3	0.81	0.28	1	1.4	2.2	1.8	2.5	2	$\Lambda^0$	620	110	0.5	0.6
31-7464	16.3	17.3	0.03	0.30	1	1	>14	1.2	<1.5	<1.5	$\theta^0$	730	690	4.5	1
31-7629	6.5	8.3	0.12	0.13	1	1	12	1.3	1	1	$\theta^0$	1800	1400	2	0.8
33-8745	13.3	15.5	0.09	0.25	1	1	>14	1.4	1	<1.5	$\theta^0$	890	750	1.2	2.2
34-9528	4.3	6.8	0.23	0.09	1	1	11	1.5	1	1	$\theta^0$	2600	1700	3.3	0.8
34-9630(A) <sup>c</sup>	6.5	8.0	0.10	0.13	1	1	>14	1.2	1	1	$\theta^0$	1800	1500	1.8	2.3
34-9630(B) <sup>c</sup>	5.8	6.5	0.06	0.11	1	1	>>14	1.4	1	1	$\theta^0$	2000	1800	1.0	1
34-9972	5.5	14.0	0.44	0.14	1	1	2.4	1.1	3	1	$\Lambda^{0*}$	590	230	1.5	1.3
34-9995	32.3	51.3	0.33	0.84	1	1	>>14	1.8	1	1	$\theta^0$	370	250	5	5
35-0343	11.5	12.5	0.04	0.21	1	1	>14	1.4	1	1	$\theta^0$	1000	940	1.5	0.6
35-0707	10	11	0.05	0.18	1	1	>14	1.4	1-1.5	1.5-2	$\theta^0$	1200	1100	2.1	1.2
35-0766	13.5	44.5	0.61	0.39	1	1.1	3.8	1.4	3	1.5	$\Lambda^0$	420	140	4	3
36-1131	14	20	0.19	0.30	1	1	11	1.1	1.5	1	$\theta^0$	820	580	3	0.4
37-1869	5.3	10.5	0.34	0.12	1	1	4	1.1	1	1	$\theta^0$	2000	1000	1	0.5
38-2438	46.5	62.5	0.29	1.36	1	1.1	>>14	1	1	1	$\theta^0$	280	230	1	1
38-2494	15.0	41.0	0.53	0.41	1	1	4.8	1.4	2-2.5	1	$\Lambda^0$	360	140	4	2
38-2506	2.0	5.0	0.43	0.05	1	1	2	1	1.5-2	1	$\Lambda^{0*}$	670	270	0.1	0.5
38-2954	6.0	9.0	0.21	0.13	1	1	8.8	1.2	1	1	$\theta^0$	1900	1300	0.5	1
38-2976	12.0	16.5	0.16	0.25	1	1	12	1.1	1	1	$\theta^0$	960	700	4	2
40-4526	5.0	8.0	0.23	0.12	1	1	6.7	1.2	1.5-2	1.5-2	$\theta^0$	2200	1400	1.5	1.3
44-8014	6.0	8.5	0.17	0.12	1	1	11	1.3	1	1	$\theta^0$	1900	1400	0.3	1.1
U2-0938	11.0	16.3	0.20	0.23	1	1	11	1.4	1	1	$\theta^0$	1000	710	4	2
U3-1485	9.3	11.5	0.11	0.18	1	1	>14	1.4	1	1	$\theta^0$	1300	1000	0.1	0.8
U4-2176	20.5	24.5	0.10	0.41	1	1	>14	1.5	1	1	$\theta^0$	580	490	2	1
U4-2251	11.0	63.5	0.82	0.35	1	1.5	3.0	2	2.5	1.5	$\Lambda^0$	500	110	5	3
U4-2300	18.0	57.8	0.66	0.54	1	1.1	6	1.8	1	1.5	$\theta^0$	520	190	2.3	1.7
U4-2395	12.3	29.5	0.45	0.31	1	1	4.4	1.2	1	1	$\theta^0$	830	360	3	2
U4-2590	8.0	8.5	0.04	0.15	1	1	>14	1.5	1	1	$\theta^0$	1500	1400	1.8	0.3
U7-4253	12.5	20.0	0.24	0.28	1	1	9	1.3	1-1.5	1-1.5	$\theta^0$	900	570	2.5	1.3
U9-5775	13.5	26.8	0.35	0.33	1	1	6.0	1.3	6	1.5	$\Lambda^0$	310	160	5.5	1
U9-6000	8.0	17.0	0.37	0.19	1	1	4.3	1.2	1	1	$\theta^0$	1300	630	0.8	0.9
U11-7302	8.5	39.5	0.69	0.25	1	1.1	2	1.3	1.5-2	1-1.5	$\Lambda^{0*}$	680	160	4	2
U13-9043	7.5	14.0	0.31	0.17	1	1	5.5	1.2	1	1	$\theta^0$	1500	780	2	1
U21-5050	28.0	30.0	0.04	0.55	1	1	>14	1.6	1	1-1.5	$\theta^0$	430	410	Extreme	Orientation
U22-5825	18.0	31.0	0.30	0.42	1	1	9.4	1.4	1	1	$\theta^0$	620	380	2	1.3
U23-6891	7.0	28.0	0.62	0.20	1	1	1.6	1.1	1.5-2	1-1.5	$\Lambda^{0*}$	800	210	0	0.5
7-9323	5.5	5.8	0.02	0.10	1	1	>14	1.8 $\pi$	>>14	3	Anom	...	...	3.1	1.3
8-9973	3.8	11.5	0.51	0.10	1	1	1.2	1 $\pi$	1	3	Anom	...	...	2.2	0.3
9-4708	9.3	36.3	0.64	0.27	1	1	2.2	1.1 $\pi$	<1.5	<3	Anom	...	...	2.5	1
16-5707	2.0	21.5	0.84	0.06	1	1.4	1	1.5 $\pi$	1-2	2-4	Anom	...	...	2.2	1
17-6952	2.5	20.0	0.79	0.08	1	1.1	1	1 $\pi$	1-2	<4	Anom	...	...	3.7	1.8
20-8736	3.3	11.3	0.56	0.09	1	1	1	1.1 $\pi$	>14	1.5	Anom	...	...	4	2
21-9644	11.3	16.5	0.19	0.24	1	1	12	1.0 $\pi$	>>14	3.5	Anom	...	...	4	2
22-0633	10.3	44.5	0.69	0.31	1	1.1	2.6	1.4 $\pi$	1	3	Anom	...	...	4	1.5
44-7851	32	38.5	0.12	0.70	1	1	>14	1.6 $\pi$	2	1	Anom	...	...	...	...
U1-0374	6.0	23.5	0.61	0.17	1	1	1.5	1.1 $\pi$	1	3	Anom	...	...	0	0.5
U8-5672	4.0	35	0.82	0.13	1	1.5	1.2	1.4 $\pi$	1-1.5	2.5	Anom	...	...	...	...
U9-5993	7.5	27.5	0.60	0.21	1	1	1.9	1.2 $\pi$	1.5	2.5	Anom	...	...	2.5	0.8
U23-6862	4	27.5	0.76	0.12	1	1.1	1.1	1.1 $\pi$	1-1.5	3	Anom	...	...	...	...

\* See text for the definitions of the certain, starred, and anomalous events.

<sup>b</sup>  $\alpha$  has either (+) or (-) sign (i.e., equally probably) for all  $\theta^0$ -decay events but only (-) sign for the present  $\Lambda^0$ -decay cases.<sup>c</sup> Events (34-9630A, B) are two  $\theta^0$  particles which appear to come from the same penetrating shower origin.

$\alpha$  have been tried also for the starred events and anomalous cases.

A summary of the results of classification for the 129 shower-associated  $V^0$  events is given in Table IV. It is seen that 23 events have been classified as due to the decay of  $\Lambda^0$  particle, 39 as due to  $\theta^0$  particles, and 13 as anomalous events. In addition, there are 11 nonclassified events and 16 events with rather poor origins, neither of which are listed in Table III, and 27 events of nonmeasurable origins.

## 2. Simple Method

This method may be called "ionization-momentum-ionization" method to distinguish it from the " $\alpha$ - $\epsilon$  ionization" method, and is a much quicker method for checking those cases where the ionization can be fairly accurately estimated (e.g.,  $I/I_{\min} \simeq 2-6$ ). One starts out by calculating  $p_1/p_2 = \sin\phi_2/\sin\phi_1$ , which is true for any two-body decay scheme. By using one of the two estimated ionizations, say  $I_1/I_{\min}$ , two possible values of  $p_1$  (for a proton and a pion) are found for the two possible decay schemes, and hence two possible values of  $p_2$  from the above ratio. Consequently, two possible values of  $I_2/I_{\min}$  are obtained from the ionization-momentum curves and can be then compared with the observed  $I_2/I_{\min}$ . As an example we take the event (27-4019). Here,  $p_1/p_2 = \sin\phi_2/\sin\phi_1 = 3.1$ . The observed  $I_1/I_{\min}$  and  $I_2/I_{\min}$  are, respectively, about 3 and 1.5. We assume first  $\theta^0 \rightarrow \pi^+ + \pi^-$ . Then the corresponding  $p_1$  is found to be about 75 Mev. Hence  $p_2 = 75/3.1 \simeq 24$  Mev, and the corresponding  $I_2/I_{\min}$  is found to be greater than 14. Therefore, this event cannot be a  $\theta^0$ -decay event. Let us assume next that  $\Lambda^0 \rightarrow p + \pi^-$ . Then  $p_1$  (proton) corresponding to  $I_1/I_{\min} \simeq 3$  is about 500 Mev, and  $p_2$  (pion) =  $500/3.1 \simeq 160$  Mev for which  $I_2/I_{\min}$  is about 1.4 in good agreement with the observed value  $\sim 1.5$ . Therefore, this event is very probably due to a  $\Lambda^0$  particle. The  $\alpha$ - $\epsilon$  ionization method leads to the same conclusion. This simple method has been used to check the classification for many of the events, including all the starred cases, nonclassified events, and anomalous cases.

## 3. Ratio $N_{\theta^0}/N_{\Lambda^0}$

In order to obtain the corrected numbers for the  $\theta^0$  and  $\Lambda^0$  particles and hence a value for the ratio, corrections for the different bias effects have to be considered. For example, in the first place, each event should be weighted so that account can be taken of the particles which undergo decay before entering and after leaving the illuminated region. The weighting factor thus depends on the momentum and the mean lifetime of the  $V^0$  particle. Secondly, the detection may have different biases for the two types of particles, particularly at low energies. Specifically, the number of low-energy particles having decayed in the plate is unknown and may be different for the two types of particles. Finally,

TABLE IV. Summary of results of classification of the 129 shower-associated  $V^0$  events.<sup>a-c</sup>

Type of events	$\Lambda^0$	$\theta^0$	Anomalous
Certain	17	38	12
Starred	6	1	1

<sup>a</sup> See text for the definitions of the certain, starred, anomalous, and nonclassified events.

<sup>b</sup> In addition, there are 11 nonclassified events, which may be either  $\theta^0$  or  $\Lambda^0$  particles; and 16 events have such large uncertainty in their origins that the classification can hardly be meaningful, though their origins are measurable and have been located (with large "circle of uncertainty," of course).

<sup>c</sup> 27 cases, the rest of the 129 events, have unmeasurable origins, though they are seen to be associated with penetrating shower particles.

the uncertainties in the classification should also be considered.

We have weighted each of our  $V^0$  events in Part II; namely, we have corrected each event for the decay in the plates and that outside the useful part of the chamber. The values of the weighting factor  $W$  are shown in the last columns of Tables I and II in Part II. The uncorrected and corrected numbers of  $\theta^0$  and  $\Lambda^0$  particles are given in Table V with and without the starred cases. The standard deviations given for the corrected numbers in the last two columns have been calculated from  $(\sum_r W_r^2)^{1/2}$ . As is seen, the corrected numbers of  $\theta^0$  and  $\Lambda^0$  particles are, respectively, 106 and 52, giving a value of  $2 \pm 1$  for the ratio  $N_{\theta^0}/N_{\Lambda^0}$ , which is practically the same as the ratio of the two uncorrected numbers. The weighting done in Part II does not include the correction for the decay in the core of the penetrating shower, which is difficult to estimate.

Our observed ratio is therefore greater than obtained by previous workers.<sup>8-11</sup> However, our ratio seems to be compatible with the recent observation of "pair" production of  $V^0$  events,<sup>12</sup> where pairs of two  $\theta^0$  particles

TABLE V. Observed production ratio of  $\theta^0$  to  $\Lambda^0$  particles.

	Uncorrected number		Corrected number <sup>a</sup>	
	Including starred cases	Excluding starred cases	Including starred cases	Excluding starred cases
$\theta^0$	39 $\pm 6$	38 $\pm 6$	106 $\pm 31^b$	105 $\pm 31^b$
$\Lambda^0$	23 $\pm 5$	17 $\pm 4$	52 $\pm 18^b$	43 $\pm 17^b$
$N_{\theta^0}/N_{\Lambda^0}$	1.7 $\pm 0.6$	2.2 $\pm 0.9$	2.0 $\pm 1.3$	2.4 $\pm 1.4$

<sup>a</sup> The corrected numbers for the  $\theta^0$  particles include only 35 events, for which the weighting factors can be calculated. The other four have values of  $l < 0.4$  cm. For definition of  $l$  refer to Part II.

<sup>b</sup> Each of these errors has been calculated from  $(\sum_r W_r^2)^{1/2}$ .

<sup>8</sup> D. B. Gayther, Phil. Mag. **45**, 570 (1954).

<sup>9</sup> J. G. Wilson, in *Progress in Cosmic Ray Physics*, edited by J. G. Wilson (North-Holland Publishing Company, Amsterdam, 1954), Vol. II, p. 91; the ratio quoted here is about  $\frac{1}{2}$  from the experiments of several workers.

<sup>10</sup> D. B. Gayther and C. C. Butler, Phil. Mag. **46**, 467 (1955).

<sup>11</sup> D. B. Gayther, Phil. Mag. **46**, 1362 (1955).

<sup>12</sup> Fowler, Shutt, Thorndike, and Whittemore, Phys. Rev. **93**, 961 (1954); Ballam, Hodson, Martin, Rau, Reynolds, and Treiman, Phys. Rev. **97**, 245 (1955), and the references given there; Fretter, May, and Nakada, Phys. Rev. **89**, 168 (1953); J. D. Sorrels (reported by C. D. Anderson) *Proceedings of the Fifth Annual Rochester Conference on High Energy Physics* (Interscience Publishers, Inc., New York, 1955), p. 90.

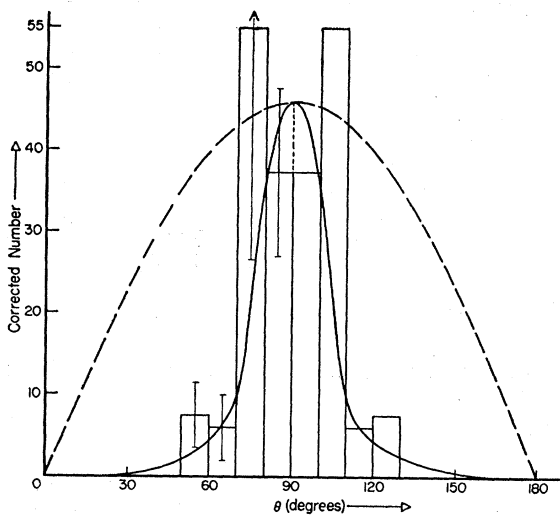


FIG. 4. Distribution of  $\theta$ , the angle of emission of the decay products of  $\theta^0$  particles in the rest system. Here the dotted curve represents the  $\sin\theta$  distribution, i.e., the isotropic distribution. Taking the 11 nonclassified events as  $\theta^0$  events practically does not change the distribution. Four  $\theta^0$  events, which have not been weighted due to values of  $l$  smaller than 0.4 cm and hence are not included in the curve, lie in the angular range about  $90^\circ$ . Therefore, they would have made the peak about  $90^\circ$  stronger, if they were included in the plot.

and pairs of one  $\theta^0$  particle and one  $\Lambda^0$  particle have been found but not pairs of two  $\Lambda^0$  particles.<sup>13</sup> In fact a value around unity for the above ratio has also been indicated in the magnet cloud chamber experiments<sup>14</sup> of Newth and James and of Arnold *et al.*, where the authors were concerned, on the average, with higher momenta of the  $V^0$  particles.

One may perhaps think that we might have missed those backward  $\Lambda^0$  particles which have been observed by some workers,<sup>15</sup> and these would naturally decrease the above ratio. However, so far we have not observed any backward  $V^0$  particle decaying in the first, second, or third gas space associated with the nuclear interactions in the first, second, or third lead plate. We might have missed those (if any) decaying in the first gas space, which was often poorly illuminated, but not those in the second or third gas space. The backward  $V^0$  particles (if any) in the second and third gas spaces would have been observed as frequently as those in the

<sup>13</sup> In fact, recent experiments with the Brookhaven Cosmotron have strongly indicated the great difficulty of pair production of two  $\Lambda^0$  particles; see G. Collins, *Proceedings of the Fifth Annual Rochester Conference on High Energy Physics* (Interscience Publishers, Inc., New York, 1955), p. 139; also A. Pais and O. Piccioni, *Phys. Rev.* **100**, 1487 (1955), footnote 3.

<sup>14</sup> J. A. Newth and G. D. James, Report of the Bagnères Conference on Cosmic Radiation, 1953 (unpublished); also, D. I. Page and J. A. Newth, *Phil. Mag.* **45**, 43 (1954); Arnold, Ballam, Grisaru, McGrew, and Wyld, *Phys. Rev.* **100**, 1804 (1955).

<sup>15</sup> Fretter *et al.*<sup>12</sup> have observed only one backward  $\Lambda^0$  particle in 23  $\Lambda^0$  particles and none for  $\theta^0$  particles. Gayther and Butler<sup>10</sup> have observed 8 backward  $\Lambda^0$  particles in 28  $\Lambda^0$  particles and none for  $\theta^0$  particles.

first gas space, for the number of nuclear interactions in the second and third plates together is more than 80% of that in the first plate (see Sec. II for reason) and moreover each of the lower plates is much thinner than the first one so that backward (low energy)  $V^0$  particles (if any) would have had greater chance to emerge from the plates and decay in the gas.

Our ratio is compatible with the notion that in  $\Lambda^0$  and  $\theta^0$  pair production, the  $\theta^0$  is not subject to capture by nuclear material in the originating plate, while the  $\Lambda^0$  has a definite chance of being left behind in an unobserved hyperfragment. However, our result that  $\theta^0$  particles may be produced as abundantly as or more abundantly than  $\Lambda^0$  particles must be taken only as a preliminary indication, because the statistics are still low and perhaps some unknown biases might have been present in observing and selecting the events for analysis, though at present we cannot think of any.

## VI. OTHER RESULTS

1. *Angle  $\delta$ .*—The study of the angle  $\delta$ , the angle between the line of flight of  $V^0$  particle and its decay plane for our classified events, suggests that the decays are of two-body type. The  $\delta$  values were measured for all these cases and are presented in Table III.

2. *Angular Distribution in the Rest System.*—As is known, in the two-body decay process the emission of the secondary particles is isotropic in the rest system of the  $V^0$  particle, if the spin<sup>16</sup> of the  $V^0$  particle is 0 or  $\frac{1}{2}$ . In order to get some information about the spin of the  $V^0$  particle, we have plotted the experimental points as shown in Figs. 3(a) and 3(b). To obtain more accurate angular distributions, we have taken into account the weighting factors  $W$  for the individual  $\theta^0$  and  $\Lambda^0$  events as has been calculated in Part II and discussed in Sec. V3.

In the decay of the  $\Lambda^0$  particles, 4 events lie in the angular region of  $0^\circ$ – $90^\circ$  in the  $\alpha$ – $\epsilon$  plot with  $\theta$ , the angle of emission of the proton in the rest system, as a parameter, and 19 lie in the region  $90^\circ$ – $180^\circ$ . However, considering the detection biases of the chamber as explained before, the corrected number of  $\Lambda^0$  events lying in region  $0^\circ$ – $90^\circ$  is 21 and that of the events lying in  $90^\circ$ – $180^\circ$  is 32; considering all the 11 nonclassified cases as due to the decay of  $\Lambda^0$  particles practically does not change this distribution. Therefore, because of low statistics and of the general trend of the distribution, no real asymmetry can be claimed.

<sup>16</sup> S. B. Treiman *et al.*, *Phys. Rev.* **97**, 244 (1955); J. Ballam *et al.*, *Phys. Rev.* **97**, 245 (1955); J. D. Sorrels, *Proceedings of the Fifth Annual Rochester Conference on High Energy Physics* (Interscience Publishers, Inc., New York, 1955), p. 90; B. Rossi, *Proceedings of the Fifth Annual Rochester Conference on High Energy Physics* (Interscience Publishers, Inc., New York, 1955), p. 125; G. Reynolds, *Proceedings of the Fifth Annual Rochester Conference on High Energy Physics* (Interscience Publishers, Inc., New York, 1955), p. 98; R. Gatto, *Nuovo cimento* **4**, 841 (1955).

As to the  $\theta^0$  decay, the indication of the departure from an isotropic distribution appears to be quite strong. The distribution for  $\theta^0$  particles is presented by the histogram in Fig. 4. The standard deviations have been calculated as before from  $(\sum_r W_r^2)^{\frac{1}{2}}$  (summing over the number of events in each angular interval) and are indicated by the vertical lines. The dashed curve in the figure represents the  $\sin\theta$  distribution, i.e., the isotropic distribution. Taking the 11 nonclassified cases as due to  $\theta^0$  particles does not affect the distribution.

It is rather difficult to see how this departure of the observed distribution from isotropy can be explained except by taking  $J \gtrsim 1$ . It may be of interest to make an estimate for the spin of the  $\theta^0$  particle, using the

relation<sup>17</sup>

$$J \gtrsim 1/(2\Delta\theta)$$

as deduced from the uncertainty principle. Here  $\Delta\theta$  is taken as the total width at half-intensity of the angular distribution as estimated from Fig. 4. Such an estimation gives  $J \gtrsim 1$ .

However, this indication of higher spin for  $\theta^0$  particles may be regarded only as a preliminary indication, because the statistics are still low and because there might be some unknown biases which we cannot trace at present.

<sup>17</sup> We should like to thank Dr. D. C. Peaslee for his helpful discussion on the estimation of the spin of the  $V^0$  particle from the angular distribution of the decay products in the rest system, and for his comment on the ratio  $N_{\theta^0}/N_{\Lambda^0}$ .

PHYSICAL REVIEW

VOLUME 106, NUMBER 1

APRIL 1, 1957

## Double-Plate Cloud-Chamber Study of $V^0$ Particles: Mean Lifetimes of $\theta^0$ and $\Lambda^0$ Particles\*†‡

ALLEN L. SNYDER, W. Y. CHANG, AND ISHWAR C. GUPTA  
*Physics Department, Purdue University, Lafayette, Indiana*

(Received February 10, 1956; revised manuscript received December 26, 1956)

The mean decay times of 35  $\theta^0$  particles and 23  $\Lambda^0$  particles have been calculated according to the maximum-likelihood procedure as discussed by Bartlett. For each event, the decay length, the "total potential" decay length and the "plate-potential" decay lengths were measured with the usual caution. The velocity of each  $V^0$  particle was determined from the  $\alpha-\epsilon$  plots, and used to convert decay lengths into the corresponding decay times in the rest system. The mean decay time for the 35  $\theta^0$  particles is found to be  $(0.8_{-0.2}^{+0.4}) \times 10^{-10}$  sec, and for the 23  $\Lambda^0$  particles  $(2.8_{-0.7}^{+1.2}) \times 10^{-10}$  sec. The differential momentum distributions of the  $\theta^0$  and  $\Lambda^0$  particles are obtained and appear to be different in shape and momentum range for the two types of  $V^0$  particles. The mean detection probability of our chambers has also been studied as a function of the momentum of the  $V^0$  particles.

### I. INTRODUCTION

THE mean decay times for  $\theta^0$  and  $\Lambda^0$  particles have been determined by several workers.<sup>1</sup> However, for either type of particle the experimental values for the mean lifetime vary considerably. For example, in the case of  $\Lambda^0$  particles they lie in the wide range (1 to 10)  $\times 10^{-10}$  sec, while for  $\theta^0$  particles they vary from about  $1 \times 10^{-10}$  sec to  $4 \times 10^{-10}$  sec. This is partly due to the fact that the statistics have been very low, particularly for  $\theta^0$  particles, and partly because there has not been a single acceptable method of measure-

ment and of analysis. In 1952, Wilson and Butler<sup>2</sup> suggested how the quantities involved in this problem should be measured, and that the maximum-likelihood procedure should be followed to deduce the lifetime. Some of the ideas have already been incorporated in one way or another by other authors<sup>1</sup> in their work. Recently Bartlett<sup>3</sup> has described, from general statistical consideration, the maximum-likelihood procedure for the evaluation of the lifetime of unstable particles observed in a magnet or multiplate cloud chamber. This procedure has been applied by Page and Newth<sup>1</sup> and by Gayther<sup>1</sup> to the estimation of the mean decay times of the  $V^0$  particles.

We have adopted the general methods of measurement as discussed by Wilson and Butler and used by other workers and the statistical procedure put in a more convenient form by Bartlett to determine the mean decay times of our  $\theta^0$  and  $\Lambda^0$  particles, which have

\* Material in this paper forms part of the material of Allen L. Snyder's Dissertation for the Degree of Doctor of Philosophy to be submitted to the Graduate School of Purdue University.

† Supported in part by the Purdue Research Foundation.

‡ Reported partly at the 1955 Thanksgiving Meeting of the American Physical Society held at Chicago [Phys. Rev. **100**, 1264(A) (1955)]; also at the Washington Meeting, April, 1956 [Bull. Am. Phys. Soc. Ser. II, **1**, 186 (1956)].

<sup>1</sup> For examples: Leighton, Wanlass, and Anderson, Phys. Rev. **89**, 148 (1953); Fretter, May, and Nakada, Phys. Rev. **89**, 168 (1953); Bridge, Peyrou, Rossi, and Safford, Phys. Rev. **91**, 362 (1953); D. I. Page and J. A. Newth, Phil. Mag. **45**, 38 (1954); D. B. Gayther, Phil. Mag. **45**, 570 (1954).

<sup>2</sup> J. G. Wilson and C. C. Butler, Phil. Mag. **43**, 993 (1952).

<sup>3</sup> M. S. Bartlett, Phil. Mag. **44**, 249, 1407 (1953).

FIG. 2. Example of the production of a  $V^0$  particle in the second lead plate. The particle decays in the third gas space. The decay products are identified as proton ( $p$ ) and  $\pi^-$ .  $\Lambda^0$  has a momentum,  $P=681$  Mev/c. Event (30-6869).

